

ARTICLE OPEN



CSE reduces OTUD4 triggering lung epithelial cell apoptosis via PAI-1 degradation

Lijuan Luo^{1,2,3}, Tiao Li^{1,2,3}, Zihang Zeng^{1,2,3}, Herui Li^{1,2,3}, Xue He^{1,2,3} and Yan Chen^{1,2,3}✉

© The Author(s) 2023

Ovarian tumor family deubiquitinase 4 (OTUD4), a member of the OTU deubiquitinating enzyme, is implicated to decrease in cancer to regulate cell apoptosis. However, the role of OTUD4 in cigarette smoke induced epithelial cell apoptosis and its mechanism have not been elucidated. In this study, we showed that OTUD4 protein reduced in CSE treated mice and airway epithelial cells. OTUD4 silence aggravated cell apoptosis and emphysematous change in the lung tissue of cigarette smoke extract (CSE) treated mice. Additionally, restoration of OTUD4 in the lung of mice alleviated CSE induced apoptosis and emphysematous morphology change. The effect of OTUD4 on cell apoptosis was also confirmed in vitro. Through protein profile screening, we identified that OTUD4 may interact with plasminogen activator inhibitor 1 (PAI-1). We further confirmed that OTUD4 interacted with PAI-1 for de-ubiquitination and inhibiting CSE induced PAI-1 degradation. Furthermore, the protective role of OTUD4 in airway epithelial cells apoptosis was blocked by PAI-1 deactivation. Taken together, our data suggest that OTUD4 regulates cigarette smoke (CS)-triggered airway epithelial cell apoptosis via modulating PAI-1 degradation. Targeting OTUD4/PAI-1 signaling might potentially provide a therapeutic target against the lung cell apoptosis in cigarette smoke (CS)-induced emphysema.

Cell Death and Disease (2023)14:614; <https://doi.org/10.1038/s41419-023-06131-1>

INTRODUCTION

Chronic obstructive pulmonary disease (COPD) is one of the top three causes of death worldwide [1], which is characterized by irreversible airway obstruction, accelerated lung function decline, and a heterogeneous combination of bronchitis and emphysema [2]. Aberrant inflammatory, oxidation imbalance and cellular apoptosis in the respiratory system in response to cigarette smoke (CS) are considered as main pathogenesis of COPD [3]. CS exposure has been reported to cause various type of cell death including apoptosis, necrosis and ferroptosis [4, 5]. Previous studies demonstrated that bronchial epithelial cells and animal lungs exposed to cigarette smoke extract (CSE)/CS increased cellular apoptosis, thus promoted emphysema and the development of COPD [6–8].

Ubiquitination is an important post-translational modification that maintains proteostasis via proteasome or lysosome and regulates numerous cellular processes, including autophagy, DNA damage signaling, and inflammation [9, 10]. The ubiquitin ligases and deubiquitin enzymes (DUBs) interacted with substrates to regulate its ubiquitination. Thus, DUBs are likely to modulate cellular functions, including inflammation, cell cycle arrest and cell death via targeting distinct substrates [11, 12]. Previous research has showed that CS destabilized the ubiquitin proteasome system (UPS) leading to DNA damage, cytotoxicity, and further emphysematous change [13]. What's more, CS causes a significant accumulation of poly-ubiquitinated proteins in vivo and vitro [6, 14, 15]. However, the changes of DUBs under cigarette smoke exposure and their role in CS induced COPD have not been elucidated.

Ovarian tumor family deubiquitinase 4 (OTUD4) belongs to the ovarian tumor proteases (OTUs) DUB family and is implicated to cleaves K48- and K63- linked poly ubiquitin chains [16–19]. It regulated DNA repairment, inflammation, cell proliferation, and apoptosis by specific deubiquitylation [16, 17, 20, 21]. TLR-mediated activation of NF- κ B is negatively regulated by OTUD4, and macrophages from OTUD4^{-/-} mice exhibit increased inflammatory signaling upon TLR stimulation [16]. What's more, loss of OTUD4 in Hela cells impaired stress granule formation and promoted apoptosis via activating caspase 3 [20]. In addition, a meta-analysis of GWAS studies reported that OTUD4 is associated with disease susceptibility in COPD [22]. However, whether OTUD4 is involved in smoking induced airway epithelial cell apoptosis and participates in COPD pathogenesis is interested to be investigated.

Plasminogen activator inhibitor 1 (PAI-1) is a multifunctional protein that belongs to the SERPIN superfamily of serine protease inhibitors, also known as serpine1 [23]. It is an effective inhibitor of plasminogen activators, particularly urokinase-plasminogen activator (uPA) and tissue-type plasminogen activator and binds to the LDL receptor (LRP) and vitronectin [24]. PAI-1 is involved in cell physiological activities, including cell adhesion, proliferation, migration, and viability [25]. Previous study demonstrated an antiapoptotic role for PAI-1, decreased expression of PAI-1 promotes cell apoptosis and inhibit cell proliferation [26]. Enhanced apoptosis was present in the lungs of PAI-1^{-/-} mice compare with wild-type mice, which contribute to LPS-induced acute lung injury [27].

¹Department of Respiratory and Critical Care Medicine, The Second Xiangya Hospital of Central South University, Changsha, China. ²Research Unit of Respiratory Disease, Central South University, Changsha, China. ³Diagnosis and Treatment Center of Respiratory Disease, Central South University, Changsha, China. ✉email: chenyan99727@csu.edu.cn Edited by Boris Zhivotovskiy

Received: 5 March 2023 Revised: 1 September 2023 Accepted: 6 September 2023

Published online: 19 September 2023

In this study, we identified that the decreased OTUD4 exaggerated apoptosis in the lung epithelia via increasing PAI-1 ubiquitination and degradation. Restoration of OTUD4 in mice mitigated lung cell apoptosis, thus contributed to the alleviation of emphysema morphology change in COPD. Above all, this study added preliminary evidence that CSE induced OTUD4 reduction promoted epithelia apoptosis in COPD pathogenesis.

MATERIALS AND METHODS

Human samples

Peripheral lung tissues from subjects who have been proceed with thoracic surgery at the Department of Thoracic Surgery, Second Xiangya Hospital of Central South University. COPD patients were previously diagnosed according to Global Initiative for Chronic Obstructive Lung Disease (forced expiratory volume in 1 s/forced vital capacity [FEV1/FVC] <0.7) [28]. The study was approved by the Medical Ethics Committee of the Second Xiangya Hospital of Central South University (No. 2021733). Written informed consent was obtained from all human subjects before their enrollment into the study, which was conducted in accordance with the Declaration of Helsinki.

Preparation of CSE

One full-strength cigarette (Marlboro; Longyan Tobacco Industrial Co, Ltd, Fujian, China; tar: 10 mg, nicotine: 1.1 mg, carbon monoxide: 11 mg) were combusted using a modified syringe-driven apparatus. 1 cigarette were

collected in 10 mL Dulbecco's minimum essential media (DMEM) for cell experiments. The smoke was bubbled into DMEM then filtered through a 0.2 μ m pore-size filter to sterilize and remove particulate matter and was used immediately. The 100% CSE sample was thereafter diluted with DMEM to appropriate percentages of CSE solution. CSE was freshly prepared for every experiment.

Animal procedure

The emphysema mouse model was built according to the protocol of Zhang et al. with slight modification [29]. Six-week-old, specific pathogen-free, BALB/c mice (21–23 g each) (Slyke Jingda, Hunan, China) were injected intraperitoneally with CSE or PBS at days 0, 11, and 22 (0.3 mL per injection). OTUD4 overexpress lentivirus, OTUD4 silent lentivirus (10^9 ifu/mL, GeneChem, Shanghai, China) or PBS (0.1 mL) was instilled intratracheally at day 14. Tiplaxtinin (5 mg/kg, 100 μ L diluted in DMSO, S7922, Selleck Chemicals, Texas, USA) was administered via oral gavage daily during mouse modeling [30]. Mice were randomly assigned to different groups for experimental treatment by a free online randomization tool (www.graphpad.com/quickcalcs/randomize1). The animals were sacrificed on day 28. The results were blindly analyzed by investigators. All animal care and experimental protocols were approved by the Animal Care and Use Committee of the Second Xiangya Hospital of Central South University (No. 2021789).

Lung tissue morphometry and immunohistochemistry (IHC)

Lung tissue samples were fixed in 4% formaldehyde, cut into 3.5 mm-thick sections, and stained with hematoxylin and eosin (HE). The morphology of lung tissues of mice was observed in random fields by light microscopy.

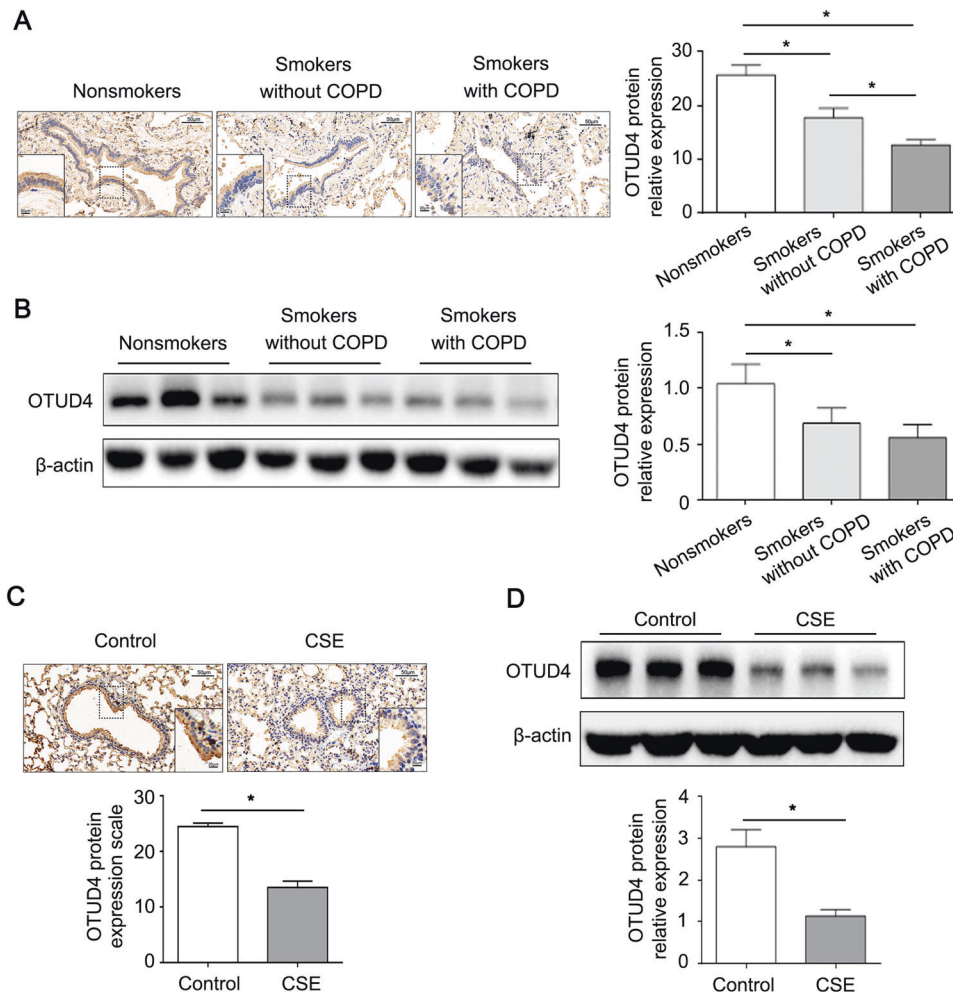


Fig. 1 OTUD4 is downregulated in the lung tissue of COPD patients and CSE-induced emphysema mouse model. **A** Representative result of IHC (400 \times magnification) for OTUD4 in human lung tissue. **B** Western blotting to detect OTUD4 protein expression in human lung tissue. **C** OTUD4 was detected with IHC in the lung tissue of mice model. **D** Western blotting was applied to detect the OTUD4 protein expression in the lung tissue of mice. Data represents as mean \pm SD of three independent experiments. * P < 0.05.

The mean linear intercept (MLI) and destructive index (DI) were measured at a magnification of 100 \times as previously described [29]. About IHC, the slides were incubated with anti-OTUD4 (1:3000, A304-605A, BETHYL). Quantitative measurements of OTUD4 positive cells in the lung tissue were performed according to previously described methods [31]. Briefly, OTUD4-positive and -negative cells were counted in each specimen. The cells positive for the OTUD4 antibody staining were expressed as a percentage of total cells. Sections were examined using a light microscope.

TUNEL assay

The TUNEL assay was analyzed according to apoptosis detection kit (Cat: # G1504, Wuhan Saiwell Biotechnology Co., Ltd, Wuhan, China). Briefly, the sections of lung tissue or cells climbing were deparaffinized in xylene and rehydrated in PBS buffer. The sections were incubated with 15 μ g/mL proteinase K for 20 min at 37 $^{\circ}$ C. After washing three times with PBS buffer, the sections were incubated in 1 \times equilibration buffer for 30 min, then incubated with a mixture containing 50 μ L of Biotin-dUTP Labeling Mix and 3 μ L of TdT Enzyme for 1 h at 37 $^{\circ}$ C in the dark. Then, the slides were incubated with 100 μ L stopping buffer for 10 min and then rinsed in PBS three times. The specimen was covered in Streptavidin-HRP for 30 min and washed in PBS three times. The slides were visualized by DAB substrate

and observed by microscope. TUNEL-positive cells were counted, and the apoptotic index was calculated as a ratio of (apoptotic cell number)/ (total cell number) in each field under magnifying view of 200 \times .

Cells and reagents

Airway epithelial cells BEAS-2b and HBE were purchased from the Chinese Academy of Sciences (Shanghai, China) and cultured in DMEM (Hyclone, Logan, UT, USA) supplemented with 10% fetal bovine serum and 50 U/mL penicillin and streptomycin (Gibco, Thermo Fisher Scientific, Waltham, MA, USA) at 37 $^{\circ}$ C in a 5% CO₂ culture chamber. Lung epithelial A549 cells were cultured in RPMI-1640 medium supplemented with 10% fetal bovine serum and 50 U/mL penicillin and streptomycin (Gibco, Thermo Fisher Scientific, Waltham, MA, USA) at 37 $^{\circ}$ C in a 5% CO₂ culture chamber. Starvation for 24 h was performed before exposure to CSE, siRNA, and/or plasmids. OTUD4 antibody (Cat: #A304-605A) was from Bethyl company (Montgomery, USA), PAI-1 (Cat: sc-5297) was from Santa Cruz Biotechnology (Shanghai, China), Bax antibody (Cat: 50599-2-Ig) was from proteintech (Rosemont, USA), BCL2 antibody (Cat: #3498) and cleaved caspase3 antibody (Cat: #9664) are from CST company (Massachusetts, USA). Lipofectamine 3000 (Cat: #L3000008) were purchased from Thermo Fisher Scientific (Waltham,

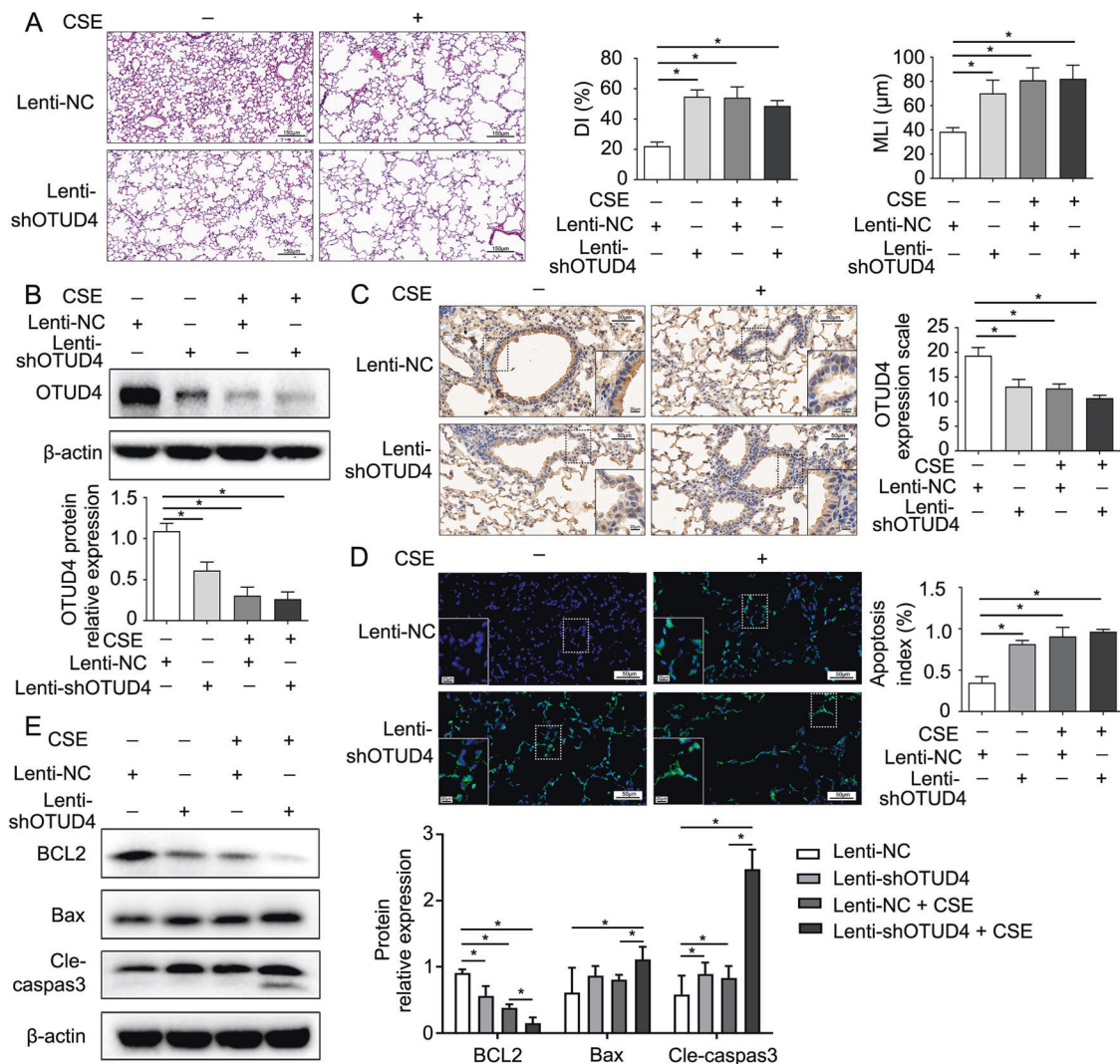


Fig. 2 OTUD4 deficiency accelerates CSE induced emphysema via increasing airway epithelium apoptosis. **A** Representative HE staining images (200 \times) of lung tissue were from control mice and OTUD4 deficiency mice. DI (%) and MLI (μ m) were measured. Immunoblotting (**B**) and IHC (**C**) were used to detect OTUD4 protein expression (400 \times). **D** Apoptosis of lung cells in indicated group of mice were detected via TUNEL assay (400 \times). Apoptosis index (apoptotic cells/ total cells, %) was calculated. **E** BCL2, Bax and cleaved-caspase 3 protein expression was detected via immunoblotting. Lenti-NC: negative control; Lenti-shOTUD4: OTUD4 knockdown. Data were shown as mean \pm SD of three independent experiments. * P < 0.05.

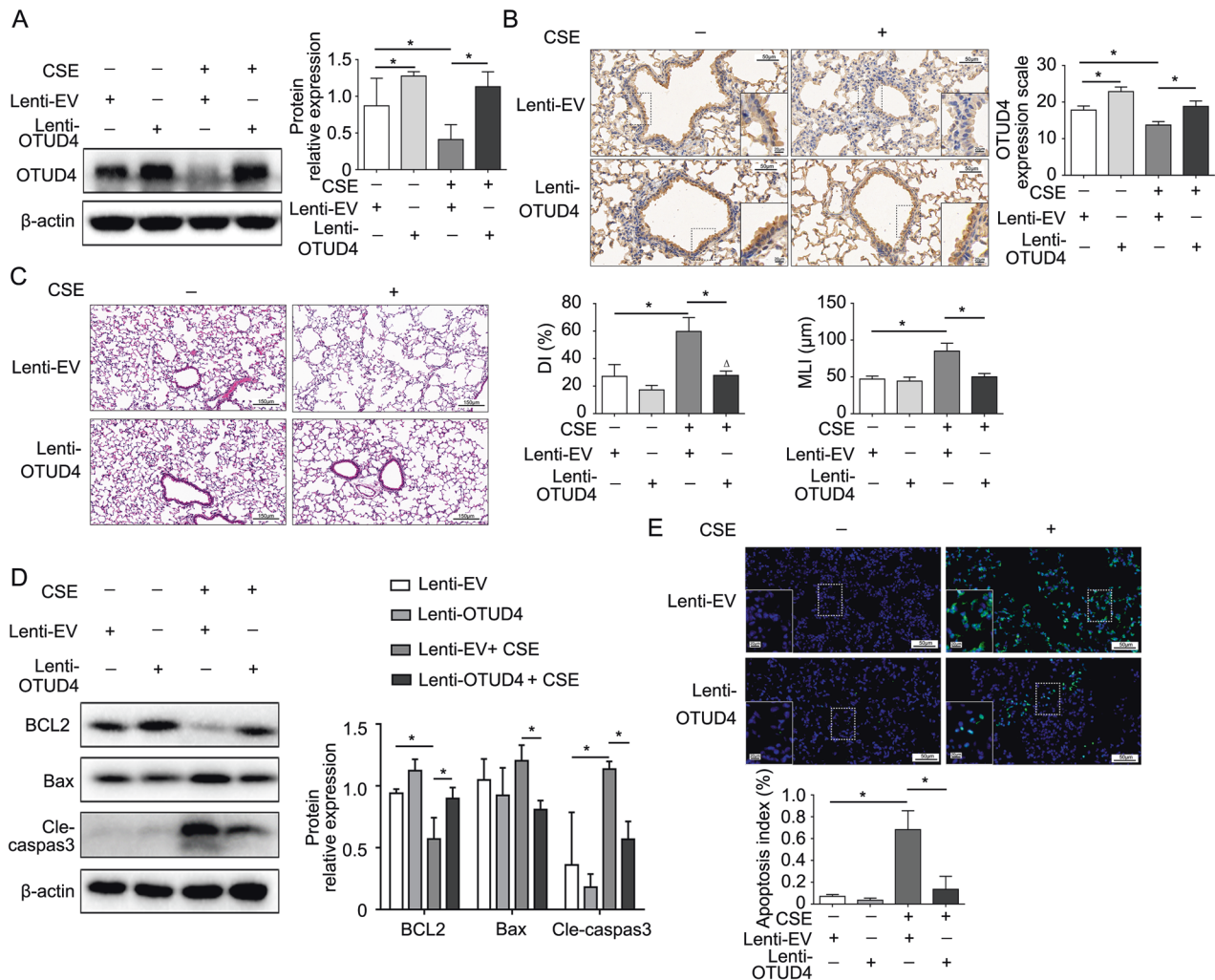


Fig. 3 Enhanced OTUD4 alleviates emphysema by reducing cell apoptosis. **A** Western blot to detect the expression of OTUD4 protein in the lung tissue of mice. **B** Representative results of IHC (400×) for OTUD4 in different groups were shown. **C** Histological changes of lung sections were shown with H&E (200×) staining. Morphometric measurements of MLI (μm) and DI (%) were plotted. **D** The expression of apoptotic protein including BCL2, Bax and cleaved caspase 3 were detected in the lung tissue of mice. **E** Apoptotic nuclei were detected by TUNEL staining (400×) in the lung tissue of mice. Lenti-EV: empty vector, Lenti-OTUD4: OTUD4 overexpression; Data were shown as mean ± SD of three independent experiments. **P* < 0.05.

MA, USA), Cycloheximide (CHX, HY-12320) and MG132 (HY-13259) were purchased from MedChemExpress (New Jersey, USA). Tiplaxtinin (S7922) was purchased from Selleck Chemicals (Texas, USA).

Protein identification by mass spectrometry

Spectra of the peptide pools were obtained on a MALDI-TOF/TOF instrument (ABI4700; Applied Biosystems). MALDI mass spectra (~100) were acquired for each digest and internally calibrated using trypsin autolysis peaks, and the top seven most abundant signals (within *m/z* 900–2,000) were automatically selected for tandem analysis. Precursor masses corresponding to a list of contaminant masses commonly observed in this laboratory were excluded from the list of precursor masses for tandem analysis. The peptide fragmentation spectra were processed using Data Explorer (version 4.5; Applied Biosystems). After centroiding and background subtraction, the spectra were used to search the National Center for Biotechnology Information nonredundant database using MASCOT (version 1.9; Matrix Sciences).

Small-interfering RNA transfection

Scramble siRNA or OTUD4 siRNA were constructed and purchased from RiboBio company (Guangzhou, China). BEAS-2b cells were transfected with scramble or OTUD4 siRNA for 48–72 h following the manufacturer's instructions. Knockdown of OTUD4 with siRNA were confirmed by RT-qPCR

and western blotting. The OTUD4 siRNA used in the experiments was as follows: GTAGCTGATGAAGATAACA.

Plasmid transfection

The plasmid vector GV362, OTUD4 overexpressed plasmids, PAI-1 overexpressed plasmids and ub-related plasmid were from GeneChem company (Shanghai, China). Briefly, 2×10^5 of BEAS-2b cells or HEK293T cells were used for each transfection. 2 μg of plasmids were transfected into BEAS-2b cells or HEK293T cells with lipofectamine 3000 for 48 h according to the manufacturer's instructions.

Western blot analysis

After stimulation, whole cell extracts were prepared using RIPA buffer [19]. Cell lysates were separated with SDS-PAGE and transferred to PVDF membrane. Then, PVDF membranes were incubated with OTUD4 antibody (1:3000), Bax antibody (1:1000), BCL2 antibody (1:1000), cleaved caspase 3 antibody (1:1000) and PAI-1 antibody (1:200) overnight. To standardize the expression of each protein, the membranes were reported with anti-β-actin antibody (1:5000). The membranes were then incubated with the appropriate peroxidase-conjugated secondary antibodies (1:5000, SA00001-1/SA00001-2, proteintech). The bound antibodies were visualized by chemiluminescence (ECL plus; GE Healthcare, Buckingham, UK).

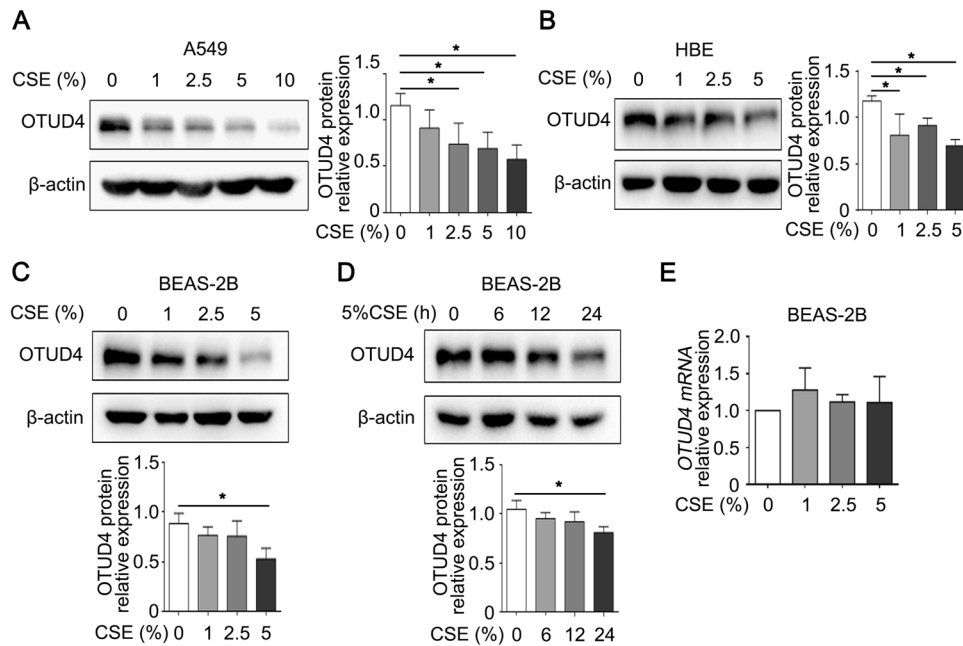


Fig. 4 OTUD4 decreases in CSE induced lung epithelial cells. A–D OTUD4 relative expression was assayed by western blotting in type II epithelial A549 cells, HBEs and BEAS-2b. E RT-qPCR to detect the mRNA level of OTUD4 in CSE treated BEAS-2b cells. Data represents as mean \pm SD of three independent experiments. $P < 0.05$.

Isolation of RNA and real-time qPCR

The total RNA was isolated from the cells using TRIZOL reagent (Invitrogen, California, USA) and then treated with DNase I (Invitrogen, California, USA) according to the manufacturer's instructions. Total RNA was then reverse transcribed using the Revert Aid First Strand cDNA Synthesis Kit (Thermo Scientific, Massachusetts, USA). Subsequently, real-time PCR was performed using a Step One Plus real-time PCR system (Life Technologies, Carlsbad, CA, USA). GAPDH was used as an internal control. The sequences of all primers used were:

OTUD4-F: 5'-AGACCCGAACCAAGCACAT-3'.

OTUD4-R: 5'-CTGGCTTTGTTCGCA-3'.

GAPDH-F: 5'-TCAAGAAGGTGGTGAAGCAG-3'.

GAPDH-R: 5'-CGTCAAAGGTGGAGGAGTG-3'.

Transcript levels were normalized to the housekeeping gene GAPDH levels. The relative mRNA levels were calculated according to the comparative Ct ($\Delta\Delta$ Ct) method, where Ct represents the threshold cycle for each transcript.

Co-immunoprecipitation

Co-immunoprecipitation (Co-IP) was conducted as previously described [32]. Briefly, 1 mg of cell lysates (in PBS with 0.5% Tween 20, and protease inhibitors) were incubated with specific primary antibodies for overnight at 4°C. The mixture was added to 40 μ L of protein A/G-agaroses for an additional 2 h at 4°C. The precipitated complex was washed three times with 0.5% Tween 20 in PBS and analyzed by immunoblotting as described above.

Ubiquitination assay

The BEAS-2b cells or HEK293T cells were co-transfected with plasmid. After incubation with 5 μ M MG132 for 5 h before harvesting, and then which they were washed with PBS and lysed with IP lysis/wash buffer with protease inhibitor and phosphatase inhibitor (Roche) and 10 μ M N-ethylmaleimide (NEM; Sigma, St Louis, MO, USA) on ice for 30 min. The cleared lysates were quantified, and an equal amount of each lysate was used for immunoprecipitation with protein A/G agarose (Sigma) pre-bound with the specified antibodies. The resin beads were washed with lysis buffer, and samples were eluted. The eluted fraction was further separated on an SDS-PAGE gel. Subsequent western blotting was performed using the indicated antibodies using the enhanced chemiluminescence-detection system (BIO-RAD, CA, USA).

Immunofluorescence staining assays

Immunofluorescence (IF) staining was conducted as previously described [33]. Briefly, cells (2×10^5) were plated at 70% confluence onto 35 mm MatTek glass-bottomed culture dishes. Immunofluorescent cell imaging was performed with a Nikon A1 confocal microscope. Cells were washed with PBS and fixed with 4% paraformaldehyde for 20 min, then exposed to 15% BSA, 1:500 dilutions of primary antibodies, and 1:1000 dilutions of Alexa-488- or Alexa-647-labeled goat anti-mouse or anti-rabbit secondary antibodies sequentially for immunostaining.

Statistical analysis

All of the statistical tests were performed using SPSS 23.0. The data are presented as mean \pm SD, or as counts or percentages as relevant. Two-group comparisons were performed using an independent sample t-test. Multiple groups were compared using one-way ANOVA. Statistical significance is denoted by $p < 0.05$.

RESULTS

OTUD4 is reduced in the lung tissue of COPD patients and emphysema mouse model

Previous research proved that DUBs are regulated by cigarette smoke [34, 35]. We firstly performed IHC to detect the expression of OTUD4 in the peripheral lung tissue specimens from nonsmokers, smokers without COPD, and smokers with COPD. The results showed that OTUD4 was widely distributed in the airway and lung epithelium, and its abundance was lower in the smoker patients with or without COPD than nonsmokers (Fig. 1A).

To confirm these results, the western blot analysis was applied and demonstrated that OTUD4 protein levels were significantly reduced in smokers with and without COPD comparing to nonsmokers (Fig. 1B). Interestingly, the OTUD4 expression was obvious reduced in the lung tissue of cigarette smoke extract induced emphysema mouse model (Fig. 1C, D). These results indicated that OTUD4 protein levels were decreased significantly in cigarette smoke-induced COPD patients and emphysema mouse model.

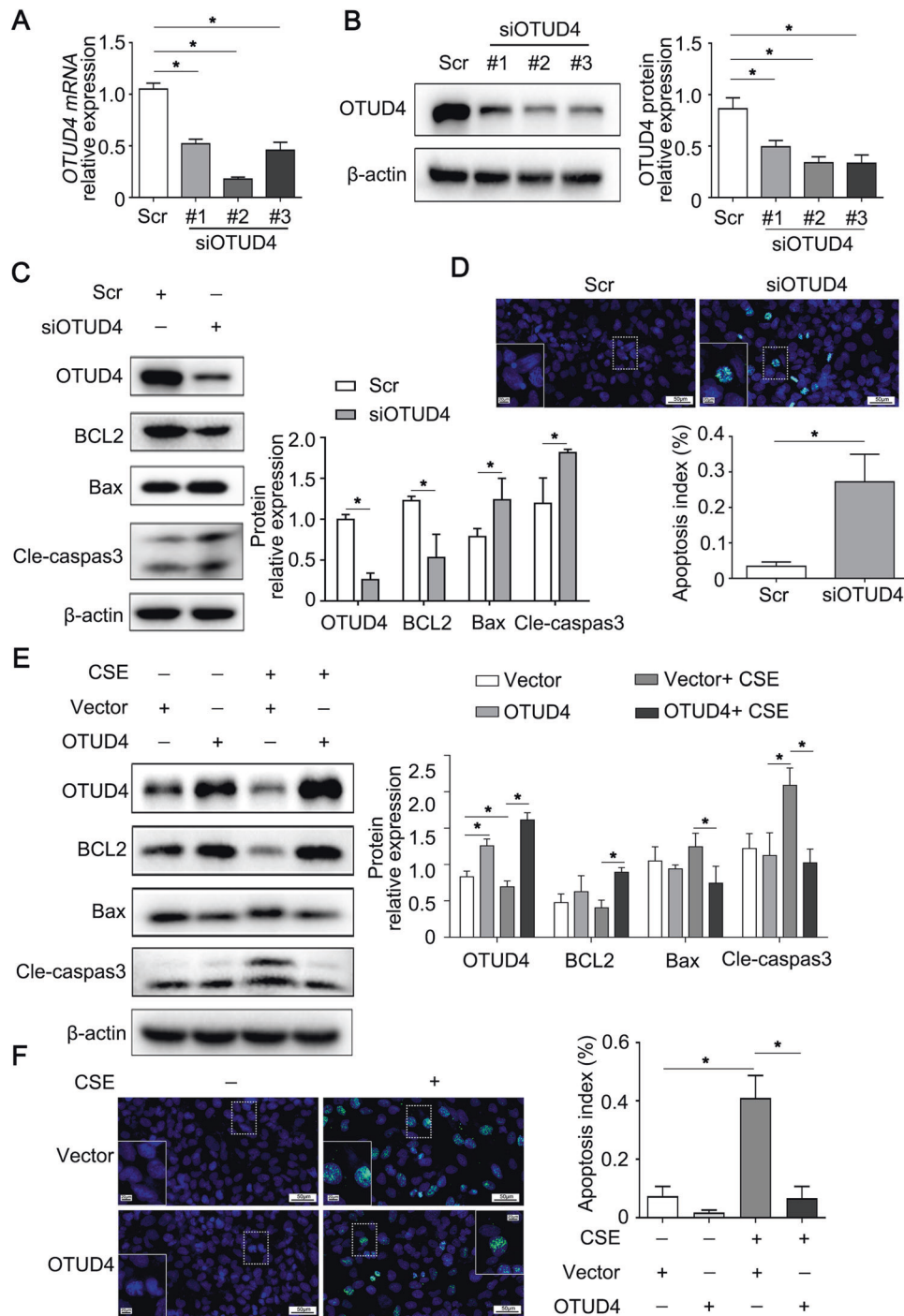


Fig. 5 OTUD4 regulates apoptosis in lung epithelial cells induced by CSE. **A, B** The mRNA and protein level of OTUD4 were confirmed with RT-qPCR and western blot. **C** OTUD4, BCL2, Bax, cleaved-caspase 3 or β -actin were assayed with western blotting after OTUD4 knockdown. **D** TUNEL staining (400 \times) to detect apoptotic nuclei of BEAS-2b cells. **E** Western blot to detect the protein level of BCL2, Bax and cleaved caspase 3. **F** Apoptotic nuclei of BEAS-2b cells were detected by TUNEL staining (400 \times). Data were shown as mean \pm SD of three independent experiments. * $p < 0.05$.

OTUD4 deficiency aggravates airway epithelium apoptosis in CSE induced emphysema

OTUD4 is reported to regulates cell death [20, 21]. To investigate the potential role of OTUD4 in the lung of mice, a CSE mediated experimental emphysema model was established with the previous described methods. HE staining exhibited that enlargement of alveolar airspaces and destruction of lung parenchyma were presented in OTUD4 knockdown and CSE

treated mice. Furthermore, the morphological indexes of emphysema including MLI and DI were dramatically increased following the reduction of OTUD4 (Fig. 2A). We found that the OTUD4 protein levels detected by western blot and IHC were decreased significantly in CSE mouse model comparing to controls (Fig. 2B, C). Interesting, in situ TUNEL assay confirmed that lack of OTUD4 enhanced the cell apoptosis in the lung tissue of CSE induced emphysema model (Fig. 2D). Besides,

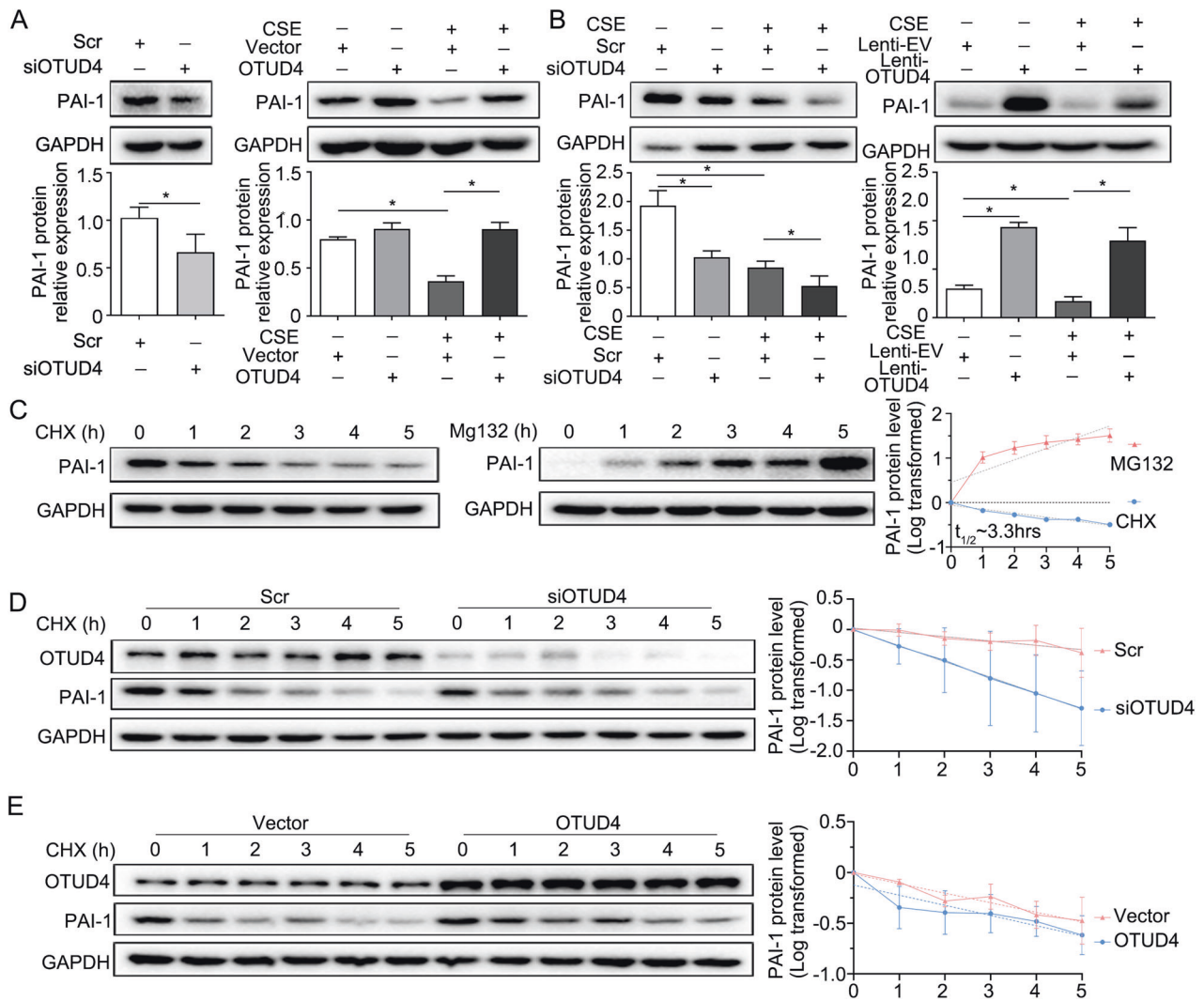


Fig. 6 OTUD4 deubiquitinates PAI-1 and inhibits its proteasomal degradation. **A** Western-blot assayed the protein level of PAI-1 in BEAS-2b cells. **B** PAI-1 protein expression in the lung tissue of mice was detected by western blotting. **C** CHX or MG132 was subjected to BEAS-2b cells. PAI-1 is with a half-life of about 3.3 h. **D, E** PAI-1 protein expression was detected by western blotting in BEAS-2b cells after OTUD4 knockdown or overexpression with CHX treatment. Data represents as mean \pm SD of three independent experiments. * $P < 0.05$.

OTUD4 knockdown increased pro-apoptotic protein Bax and Cleaved caspase 3 expression, while vigorously reduced anti-apoptotic BCL2 protein expression in lung tissue (Fig. 2E). These data illustrated that OTUD4 reduction facilitate CSE-induced emphysema in mice by increasing lung cell apoptosis.

Enhanced OTUD4 alleviates emphysema by reducing epithelia apoptosis

OTUD4 decreased in the murine lung tissue after CSE treatment and aggravated cell apoptosis. However, whether restoring the OTUD4 could protect the mice from emphysema damage is not clear. We applied OTUD4 lentivirus intratracheally to over-express OTUD4 in the lung of CSE treated mice (Fig. 3A, B). HE staining showed that enhanced OTUD4 expression partially reversed the enlargement of alveolar airspaces and destruction of lung parenchyma after CSE treatment (Fig. 3C, upper panel).

What's more, the morphological indexes of emphysema including MLI and DI were decreased after OTUD4 upregulation (Fig. 3C, lower two panels). Contrary to reduced OTUD4 expression, we proved that overexpression of OTUD4 reduced Bax and cleaved caspase 3 expression and partially reversed the

anti-apoptotic protein BCL2 expression (Fig. 3D). We further confirmed that increased OTUD4 prevented apoptosis in the lung tissue of CSE mouse model through TUNEL assay (Fig. 3E). Overall, these findings revealed that OTUD4 play a potential role in protecting CSE- induced emphysema in mice by decreasing cell apoptosis.

OTUD4 protein but not mRNA decreases in CSE treated lung epithelial cells

From above results, OTUD4 protein is mainly expressed in the airway epithelium. In order to assess the OTUD4 level under cigarette smoke treat in vitro, we analyzed the protein expression of OTUD4 in the airway and lung epithelial cells exposed to CSE. OTUD4 decreased in both A549 and HBE cell lines with a CSE dose-dependent way (Fig. 4A, B). Besides, the reduction of OTUD4 protein was further discovered in a CSE dose-dependent and time-dependent manner in the BEAS-2b cells (Fig. 4C, D). Interestingly, the mRNA level did not differ in the BEAS-2b cells exposed to different concentrations of CSE (Fig. 4E). These results indicated that the protein and mRNA expression of OTUD4 in CSE treatment is discordant.

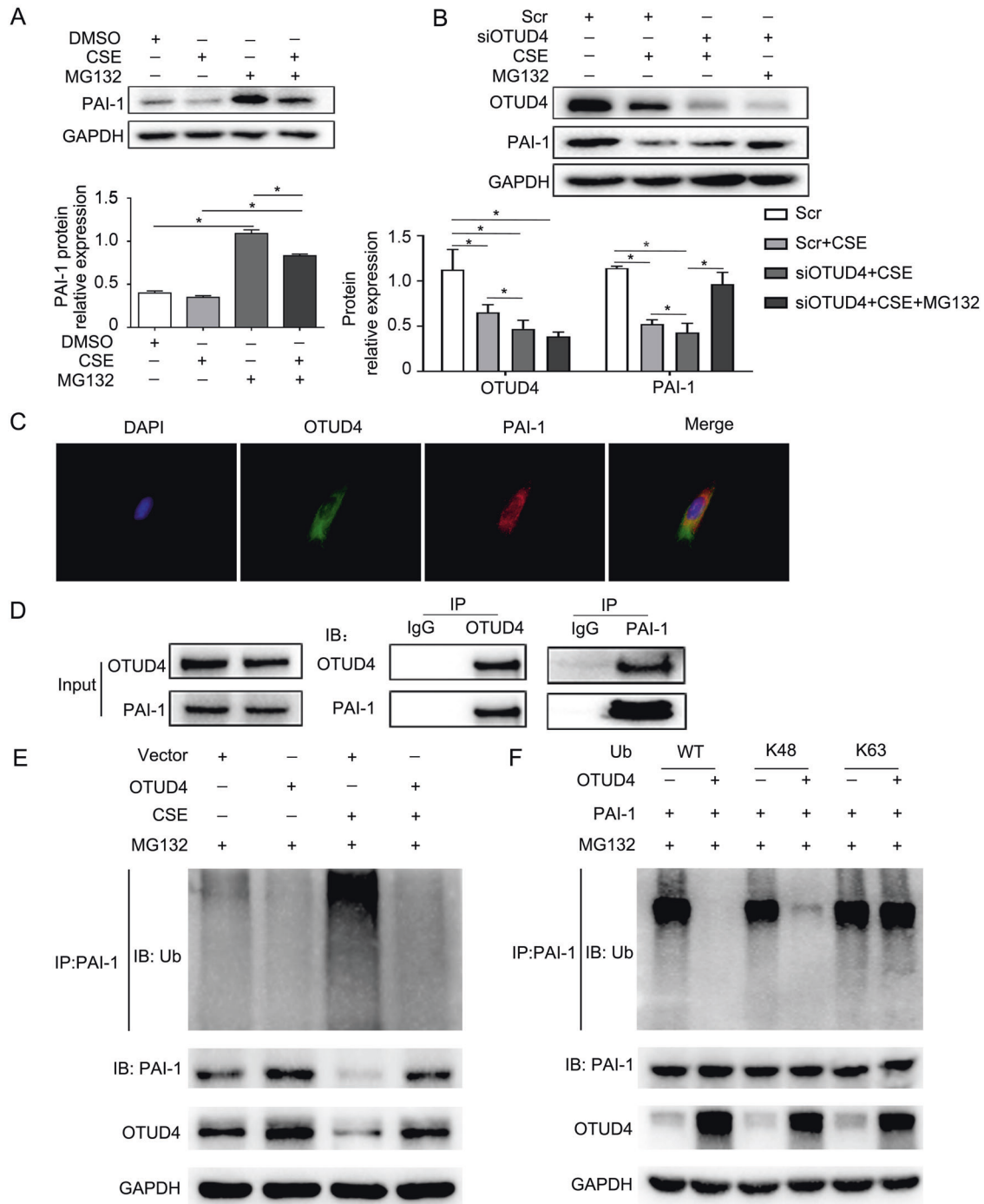


Fig. 7 OTUD4 deubiquitinates PAI-1 and inhibits its proteasomal degradation. **A, B** BEAS-2b cells were treated with CSE or MG132, CSE or MG132 was subjected to BEAS-2b cells after OTUD4 knockdown, Western blotting was used to detect OTUD4 and PAI-1 protein level. **C** Immunofluorescence staining (400 \times) of OTUD4 (green), PAI-1 (red) and DAPI (blue) and merged image (upper panel). **D** Immunoprecipitation of OTUD4 and PAI-1 (lower panel). **E** Ubiquitination assay of PAI-1 in CSE induced BEAS-2b cells after OTUD4 overexpression. **F** WT, K48, or K63 Ub was co-transfected with PAI-1 and OTUD4 into HEK293T cells. After treatment with 5 μ M MG132 for 5 h, cell lysates were subjected to ubiquitination assay. Data represents as mean \pm SD of three independent experiments. * P < 0.05.

OTUD4 regulates the apoptosis of lung epithelial cells

To confirm the above results, we next manipulate OTUD4 in BEAS-2b bronchial epithelial cells. Three strands of siRNAs targeting OTUD4 were applied to BEAS-2b cells. The second one reduced the mRNA and protein level of OTUD4 mostly, which was chosen for subsequent experiments (Fig. 5A, B). We firstly check the apoptotic protein after silence of OTUD4. As expected, we found

that lack of OTUD4 also increased the pro-apoptotic protein of Bax, cleaved caspase 3 and severely decreased the anti-apoptotic protein of BCL2 in cells (Fig. 5C). In addition, we proved that knockdown of OTUD4 enhanced cell apoptosis in BEAS-2b through the TUNEL assay (Fig. 5D). Above results further demonstrated that OTUD4 silence promoted lung epithelial cell apoptosis.

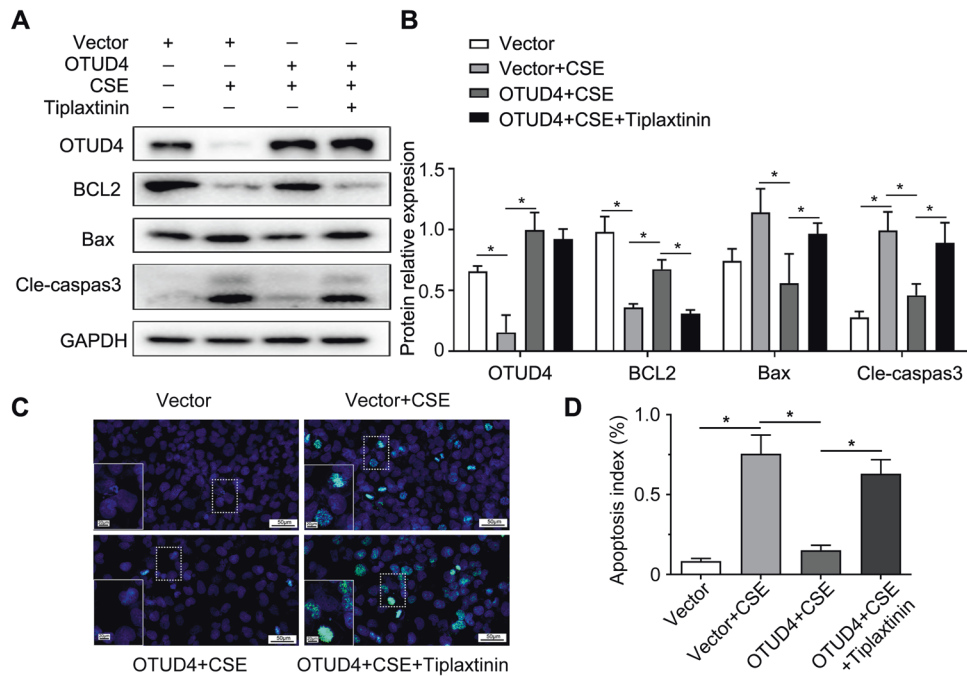


Fig. 8 Inhibition of PAI-1 perturbs the protective effect of OTUD4 on CSE induced apoptosis in BEAS-2b cells. **A** OTUD4 overexpressed cells were treated with PAI-1 inhibitor (tiplaxtinin) or CSE. OTUD4, BCL2, Bax, and Cleaved-caspase3 were detected by western blot. **B** Densitometry of OTUD4, BCL2, Bax, Cleaved-caspase3. **C** Apoptotic nuclei were detected by TUNEL staining (400 \times) in OTUD4 overexpressed BEAS-2b cells treated with CSE or tiplaxtinin. **D** Apoptotic index (%) was plotted. Data represents as mean \pm SD of three independent experiments. * $P < 0.05$.

To verify whether OTUD4 could prevent the epithelia apoptosis, we overexpressed OTUD4 in BEAS-2b cells exposed to CSE. We found that Bax and cleaved caspase 3 were reduced, while BCL2 was enhanced after CSE treatment (Fig. 5E). Furthermore, TUNEL fluorescence assay showed that the apoptosis of BEAS-2b was significantly increased under CSE stimulation. While enhanced expression of OTUD4 obviously alleviated the epithelia apoptosis after CSE exposure (Fig. 5F). As expected, these results also demonstrated that OTUD4 prevents CSE-induced apoptosis in epithelial cells.

OTUD4 deubiquitinates PAI-1 and inhibits its proteasomal degradation

How the OTUD4 regulating apoptosis is still not clear. Through protein profile screening, we found that OTUD4 may interact with protein PAI-1. Reduced OTUD4 inhibited the expression of PAI-1 protein (Fig. 6A, left panel), while overexpression of OTUD4 partially reversed the protein level of PAI-1 in CSE treated BEAS-2b cells (Fig. 6A, right panel). The same results were confirmed in the lung tissue of CSE induced emphysema mice model (Fig. 6B). Considering that OTUD4 is a deubiquitinating enzyme, we use proteasome inhibitors MG132 and protein synthesis inhibitor chlorhexidine (CHX) respectively to detected whether PAI-1 is regulated by the ubiquitin proteasome pathway. CHX-treated cells showed that PAI-1 is unstable with a half-life of approximate 3.3 h (Fig. 6C, left and right panel). In addition, PAI-1 proteins tended to increase under MG132 treatment (Fig. 6C, middle panel). This data suggested that PAI-1 was degraded via proteasome mechanism. Next, we performed CHX and MG132 in the BEAS-2b cells after modulating of OTUD4. Results showed that OTUD4 knockdown promoted PAI-1 degradation, while OTUD4 overexpression slow-down the deduction of PAI-1 expression (Fig. 6D, E).

To understand if CSE-induced PAI-1 reduction is mediated by proteasome, we applied CSE and MG132 to cells, which found that MG132 treatment rescued the PAI-1 expression in CSE treated cell

(Fig. 7A). What's more, OTUD4 silence contributed to the instability of PAI-1 induced by CSE (Fig. 7B). Further immunofluorescent staining and co-immunoprecipitation proved that OTUD4 was associated with PAI-1 (Fig. 7C, D). In addition, ubiquitination assay showed that CSE can increase ubiquitination and degradation of PAI-1, while enhanced OTUD4 expression can decrease the ubiquitination level of PAI-1 induced by CSE (Fig. 7E). And then to identify which type of ubiquitin chain of PAI-1 was affected by OTUD4, we co-transfected HEK293T cells with PAI-1, OTUD4, WT ubiquitin, K48-specific or K63-specific ubiquitin plasmid. Our results indicated that OTUD4 could efficiently remove K48-linked ubiquitin chain from PAI-1 (Fig. 7F). Taken together, OTUD4 is a specific DUB responsible for PAI-1 deubiquitination and stabilization.

Inhibition of PAI-1 perturbs the protective effect of OTUD4 on CSE induced apoptosis

In order to further prove that the protection of OTUD4 from CSE-induced apoptosis is achieved by regulating PAI-1, we used PAI-1 inhibitors, tiplaxtinin, to treat BEAS-2b cells with OTUD4 overexpression. Results showed that enhanced OTUD4 increased the expression of anti-apoptotic protein BCL2 and reduced the expression of pro-apoptotic proteins Bax and cleaved caspase3 in CSE-induced BEAS-2b cells. However, the addition of tiplaxtinin reversed the protective effect of OTUD4 and increased CSE induced cell apoptosis (Fig. 8A, B). What's more, TUNEL assay showed that apoptotic cells were decreased significantly under OTUD4 overexpression, while obviously enhanced in CSE + OTUD4+tiplaxtinin group (Fig. 8C, D).

In addition, we further confirmed these results through in vivo experiments. We performed administration of tiplaxtinin via oral gavage daily in mice with overexpression of OTUD4 under CSE intervention. We found that enhanced OTUD4 expression can improved the CSE induced emphysematous change, which include enlargement of alveolar airspaces, destruction of lung

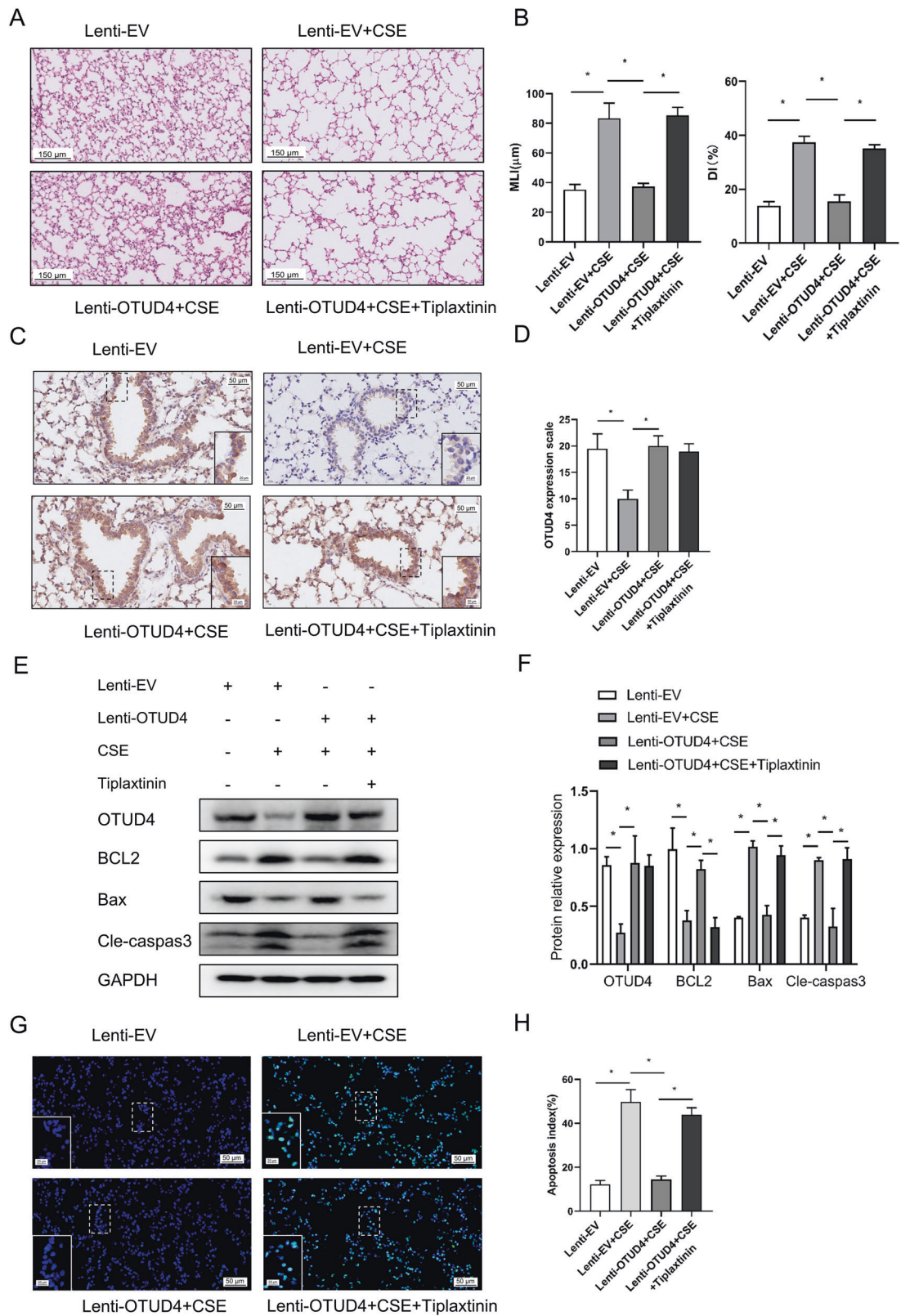


Fig. 9 Inhibition of PAI-1 perturbs the protective effect of OTUD4 on CSE induced apoptosis in lung tissue of mice. **A, B** Histological changes of lung sections were shown with H&E (200 \times) staining. Morphometric measurements of MLI (μm) and DI (%) were plotted. **C-D** Representative results of IHC (400 \times) for OTUD4 in different groups were shown. **E, F** Western blot to detect the expression of OTUD4, BCL2, Bax and cleaved caspase 3 protein in the lung tissue of mice. **G, H** Apoptotic nuclei were detected by TUNEL staining (400 \times) in the lung tissue of mice. Lenti-EV: empty vector, Lenti-OTUD4: OTUD4 overexpression; Data were shown as mean \pm SD of three independent experiments. * $P < 0.05$.

parenchyma and elevated morphological index MLI and DI. However, the treatment of tiplaxtinin can inhibit the protective effect of OTUD4 in CSE induced emphysema (Fig. 9A, B). We confirm that OTUD4 was successfully overexpressed in CSE induced emphysema mice (Fig. 9C, D). The results showed that overexpressed OTUD4 can increase the level of anti-apoptotic protein BCL2 and reduce the level of pro-apoptotic proteins Bax and cleaved caspase3 in the lung tissue of CSE induced emphysema mice. But there demonstrated opposite alternation in Lenti-OTUD4 + CSE+Tiplaxtinin group (Fig. 9E, F). Furthermore, TUNEL detection also confirmed that overexpression of OTUD4 can significantly reduce CSE induced lung cell apoptosis, while the apoptotic cells were significantly increased with tiplaxtinin treatment (Fig. 9G, H). All above inferred that OTUD4 participates in the regulation of CSE-induced apoptosis by regulating the expression of PAI-1.

DISCUSSION

In this study, we demonstrated that, (i) cigarette smoke decreased OTUD4 in cellular and mouse models; (ii) OTUD4 silencing promoted airway epithelial apoptosis induced by CSE, while OTUD4 reconstitution attenuated CSE induced apoptosis both in vivo and in vitro; (iii) OTUD4 regulated airway epithelial cell apoptosis through modulating the ubiquitination and degradation of PAI-1 protein.

COPD is a heterogeneous disease, airway inflammation, oxidative stress and cell deaths forming network module in COPD pathogenesis. Regulated cell death (RCD) play an important role in physiological processes including maintenance of homeostasis. Excess RCDs causes airway inflammation, lung tissue injury and destruction in the pathogenesis and development of COPD [36]. Epithelial cells extending from the upper airways to the terminal alveoli are the first line of defense within the lungs. Dysregulated RCDs of airway epithelial cells including apoptosis, necroptosis, pyroptosis and ferroptosis promotes emphysema and lung destruction in COPD [37–40]. Here we also confirmed that airway epithelial cell apoptosis involved in the emphysematous destruction in COPD.

Ubiquitination proteasome system (UPS) is reported to be activated in COPD, with accumulation of ubiquitinated proteins in the lungs of severe COPD subjects [14, 15]. CSE treatment of airway epithelial cells, macrophages, and mouse lung tissue significantly increased histone deacetylase 2 (HDAC2) ubiquitination and degradation, which is related to steroid tolerance in COPD patients [41]. Thus, reconstruction of deubiquitinase USP17 blocked cigarette smoke extract induced destruction of HDAC2 [42]. The deubiquitylating enzyme USP25 is implicated to decrease under smoking, thus increasing bacteria load in lung epithelial cells [34]. In our research, we also found that deubiquitination enzyme OTUD4 decreased in CSE-treated bronchial epithelial cell and emphysema mouse model, which is suggested to be involved in COPD pathogenesis. This finding might add a paradigm of that de-ubiquitination enzyme decreased under CSE treatment. Besides, this evidence supported the previous studies that cigarette smoke may stimulate the level of ubiquitination to involve in the development of COPD via increasing ubiquitin ligase and decreasing deubiquitinating enzymes.

As a deubiquitinase enzyme, OTUD4 was reported to regulate DNA damage repair, which play a role in modulating cell fate decision [20, 43]. Evidence showed that OTUD4 impaired DNA repair efficiency of non-small cell lung cancer (NSCLC) cells to regulate the cell cycle and cell apoptosis [43]. Besides, OTUD4 restrained the growth of various tumor including breast, liver, and lung cancer through activating tumor cell apoptosis [21]. Interestingly, knockdown of OTUD4 upregulated HEK293T and HeLa cell death and activated

apoptotic makers [20]. In our study, we verified that OTUD4 silencing increased airway epithelial cell apoptosis and restoration of OTUD4 attenuated the CSE induced epithelial apoptosis.

Although OTUD4 modulating cell death, the molecular mechanism of OTUD4 regulated cell apoptosis is still ambiguous. Our data indicated that OTUD4 is associated with PAI-1, a serine protease inhibitor (SERPIN), which is related to ubiquitin proteasome degradation in the regulating of cell death and was reported to promote angiogenesis and tumor cell survival by preventing apoptosis [44–49]. CSE induced ubiquitination and degradation of protein-promoted cell death of lung microvascular endothelial cells and lung fibroblasts [15] [34]. In addition, PAI-1 is reported to diminish the apoptosis of neutrophils by improving the expression of the antiapoptotic proteins [27]. The expression of PAI-1 is influenced by cigarette smoke and participated in the pathogenesis of lung diseases including COPD [50–52]. Previous study showed that PAI-1 is a downstream target that is negatively regulated by Ubiquitin-E3 Ligase RNF123, and PAI-1 knockdown reduced the proliferation and invasion of glioblastoma cell lines [48]. Likewise, we confirmed that PAI-1 is a liable protein with a half-life of 3.3 hr and is regulated by ubiquitin-proteasomal mechanism.

OTUD4 executes its physiological functions mainly through the deubiquitinating enzyme activity to antagonize a K48- or K63-linked ubiquitination [16, 18]. Here, we found that OTUD4 interacts with PAI-1 and removes its K48-linked ubiquitination. Deactivating of PAI-1 in vivo and in vitro inhibit the protective effect of OTUD4 on cell apoptosis. Our data further revealed that OTUD4 regulates epithelial cell apoptosis through governing PAI-1 ubiquitin-proteasomal degradation. Above all, we infer that OTUD4 regulated CSE induced apoptosis is related to PAI-1 de-ubiquitination and degradation.

CONCLUSION

In summary, the remarkable results of this study propose that overexpression of OTUD4 reduce cell apoptosis to protect against CSE treated lung epithelial cells and CSE mediated emphysematous model, which through PAI-1 activation. This compelling finding is helpful for understanding the pathogenesis of COPD and provide important implications on the clinical treatment of COPD in the future after further deep investigation.

DATA AVAILABILITY

The raw data acquired for the current study are available from the corresponding author upon reasonable request.

REFERENCES

- Halpin DMG, Celli BR, Criner GJ, Frith P, López Varela MV, Salvi S, et al. The GOLD Summit on chronic obstructive pulmonary disease in low- and middle-income countries. *Int J Tuberc Lung Dis.* 2019;23:1131–41.
- Heron M. Deaths: leading causes for 2008. *Natl Vital– Stat Rep. : Cent Dis Control Prev, Natl Cent Health Stat, Natl Vital– Stat Syst.* 2012;60:1–94.
- Barnes PJ, Shapiro SD, Pauwels RA. Chronic obstructive pulmonary disease: molecular and cellular mechanisms. *Eur Respir J.* 2003;22:672–88.
- Slebos DJ, Ryter SW, van der Toorn M, Liu F, Guo F, Baty CJ, et al. Mitochondrial localization and function of heme oxygenase-1 in cigarette smoke-induced cell death. *Am J Respir Cell Mol Biol.* 2007;36:409–17.
- Yoshida M, Minagawa S, Araya J, Sakamoto T, Hara H, Tsubouchi K, et al. Involvement of cigarette smoke-induced epithelial cell ferroptosis in COPD pathogenesis. *Nat Commun.* 2019;10:3145.
- Vij N, Chandramani-Shivalingappa P, Van Westphal C, Hole R, Bodas M. Cigarette smoke-induced autophagy impairment accelerates lung aging, COPD-emphysema exacerbations and pathogenesis. *Am J Physiol Cell Physiol.* 2018;314:C73–c87.
- Chen L, Luo L, Kang N, He X, Li T, Chen Y. The Protective Effect of HBO1 on Cigarette Smoke Extract-Induced Apoptosis in Airway Epithelial Cells. *Int J Chron Obstruct Pulmon Dis.* 2020;15:15–24.

8. Chen Y, Hanaoka M, Droma Y, Chen P, Voelkel NF, Kubo K. Endothelin-1 receptor antagonists prevent the development of pulmonary emphysema in rats. *Eur Respir J*. 2010;35:904–12.
9. Wu Y, Kang J, Zhang L, Liang Z, Tang X, Yan Y, et al. Ubiquitination regulation of inflammatory responses through NF- κ B pathway. *Am J Transl Res*. 2018;10:881–91.
10. Brinkmann K, Schell M, Hoppe T, Kashkar H. Regulation of the DNA damage response by ubiquitin conjugation. *Front Genet*. 2015;6:98.
11. Hanpude P, Bhattacharya S, Dey AK, Maiti TK. Deubiquitinating enzymes in cellular signaling and disease regulation. *IUBMB Life*. 2015;67:544–55.
12. Lee CS, Kim S, Hwang G, Song J. Deubiquitinases: Modulators of Different Types of Regulated Cell Death. *Int J Mol Sci*. 2021;22:4352.
13. Mallampalli RK, Li X, Jang JH, Kaminski T, Hoji A, Coon T, et al. Cigarette smoke exposure enhances transforming acidic coiled-coil-containing protein 2 turnover and thereby promotes emphysema. *JCI insight*. 2020;5:e125895.
14. Kim SY, Kim HJ, Park MK, Huh JW, Park HY, Ha SY, et al. Mitochondrial E3 Ubiquitin Protein Ligase 1 Mediates Cigarette Smoke-Induced Endothelial Cell Death and Dysfunction. *Am J Respir Cell Mol Biol*. 2016;54:284–96.
15. Min T, Bodas M, Mazur S, Vij N. Critical role of proteostasis-imbalance in pathogenesis of COPD and severe emphysema. *J Mol Med (Berl, Ger)* 2011;89:577–93.
16. Zhao Y, Mudge MC, Soll JM, Rodrigues RB, Byrum AK, Schwarzkopf EA, et al. OTUD4 Is a Phospho-Activated K63 Deubiquitinase that Regulates MyD88-Dependent Signaling. *Mol Cell*. 2018;69:505–16.e5.
17. Zhao Y, Majid MC, Soll JM, Brickner JR, Dango S, Mosammaparast N. Non-canonical regulation of alkylation damage resistance by the OTUD4 deubiquitinase. *EMBO J*. 2015;34:1687–703.
18. Liuyu T, Yu K, Ye L, Zhang Z, Zhang M, Ren Y, et al. Induction of OTUD4 by viral infection promotes antiviral responses through deubiquitinating and stabilizing MAVS. *Cell Res*. 2019;29:67–79.
19. Liu H, Fan J, Zhang W, Chen Q, Zhang Y, Wu Z. OTUD4 alleviates hepatic ischemia-reperfusion injury by suppressing the K63-linked ubiquitination of TRAF6. *Biochem Biophys Res Commun*. 2020;523:924–30.
20. Das R, Schwintzer L, Vinopal S, Aguado Roca E, Sylvester M, Oprisoreanu AM, et al. New roles for the de-ubiquitylating enzyme OTUD4 in an RNA-protein network and RNA granules. *J Cell Sci*. 2019;132:jcs229252.
21. Zhao X, Su X, Cao L, Xie T, Chen Q, Li J, et al. OTUD4: A Potential Prognosis Biomarker for Multiple Human Cancers. *Cancer Manag Res*. 2020;12:1503–12.
22. Wyss AB, Sofer T, Lee MK, Terzikhan N, Nguyen JN, Lahousse L, et al. Multiethnic meta-analysis identifies ancestry-specific and cross-ancestry loci for pulmonary function. *Nat Commun*. 2018;9:2976.
23. Chlوسی M, Carloni A, Rossi A, Poletti V. Premature lung aging and cellular senescence in the pathogenesis of idiopathic pulmonary fibrosis and COPD/emphysema. *Transl Res*. 2013;162:156–73.
24. Schar CR, Jensen JK, Christensen A, Blouse GE, Andreassen PA, Peterson CB. Characterization of a site on PAI-1 that binds to vitronectin outside of the somatomedin B domain. *J Biol Chem*. 2008;283:28487–96.
25. Li S, Wei X, He J, Tian X, Yuan S, Sun L. Plasminogen activator inhibitor-1 in cancer research. *Biomed Pharmacother*. 2018;105:83–94.
26. Wang Q, Lu W, Yin T, Lu L. Calycosin suppresses TGF- β -induced epithelial-to-mesenchymal transition and migration by upregulating BATF2 to target PAI-1 via the Wnt and PI3K/Akt signaling pathways in colorectal cancer cells. *J Exp Clin Cancer Res*. 2019;38:240.
27. Zmijewski JW, Bae HB, Deshane JS, Peterson CB, Chaplin DD, Abraham E. Inhibition of neutrophil apoptosis by PAI-1. *Am J Physiol Lung Cell Mol Physiol*. 2011;301:L247–54.
28. Vogelmeier CF, Criner GJ, Martinez FJ, Anzueto A, Barnes PJ, Bourbeau J, et al. Global Strategy for the Diagnosis, Management, and Prevention of Chronic Obstructive Lung Disease 2017 Report. GOLD Executive Summary. *Am J Respir Crit Care Med*. 2017;195:557–82.
29. Zhang Y, Cao J, Chen Y, Chen P, Peng H, Cai S, et al. Intraperitoneal injection of cigarette smoke extract induced emphysema, and injury of cardiac and skeletal muscles in BALB/C mice. *Exp Lung Res*. 2013;39:18–31.
30. Xia H, Wu Y, Zhao J, Cheng C, Lin J, Yang Y, et al. N6-Methyladenosine-modified circSAV1 triggers ferroptosis in COPD through recruiting YTHDF1 to facilitate the translation of IREB2. *Cell death and differentiation*. 2023;30:1293–1304
31. Lai T, Wu D, Chen M, Cao C, Jing Z, Huang L, et al. YKL-40 expression in chronic obstructive pulmonary disease: relation to acute exacerbations and airway remodeling. *Respir Res*. 2016;17:31.
32. Li T, Fanning KV, Nyunoya T, Chen Y, Zou C. Cigarette smoke extract induces airway epithelial cell death via repressing PRMT6/AKT signaling. *Aging*. 2020;12:24301–17.
33. Zou C, Ellis BM, Smith RM, Chen BB, Zhao Y, Mallampalli RK. Acyl-CoA:lysophosphatidylcholine acyltransferase I (Lpcat1) catalyzes histone protein O-palmitoylation to regulate mRNA synthesis. *J Biol Chem*. 2011;286:28019–25.
34. Long C, Lai Y, Li T, Nyunoya T, Zou C. Cigarette smoke extract modulates *Pseudomonas aeruginosa* bacterial load via USP25/HDAC11 axis in lung epithelial cells. *Am J Physiol Lung Cell Mol Physiol*. 2020;318:L252–L63.
35. Liu Q, Xu WG, Luo Y, Han FF, Yao XH, Yang TY, et al. Cigarette smoke-induced skeletal muscle atrophy is associated with up-regulation of USP-19 via p38 and ERK MAPKs. *J Cell Biochem*. 2011;112:2307–16.
36. Sauler M, Bazan IS, Lee PJ. Cell Death in the Lung: The Apoptosis-Necroptosis Axis. *Annu Rev Physiol*. 2019;81:375–402.
37. Aoshiba K, Yokohori N, Nagai A. Alveolar wall apoptosis causes lung destruction and emphysematous changes. *Am J Respir Cell Mol Biol*. 2003;28:555–62.
38. Chen Q, Nwozor KO, van den Berge M, Slebos DJ, Faiz A, Jonker MR, et al. From Differential DNA Methylation in COPD to Mitochondria: Regulation of AHRR Expression Affects Airway Epithelial Response to Cigarette Smoke. *Cells*. 2022;11:3423.
39. Mo R, Zhang J, Chen Y, Ding Y. Nicotine promotes chronic obstructive pulmonary disease via inducing pyroptosis activation in bronchial epithelial cells. *Mol Med Rep*. 2022;25:92.
40. Dera AA, Al Fayi M, Otifi H, Alshyarba M, Alfilhi M, Rajagopalan P. Thymoquinone (Tq) protects necroptosis induced by autophagy/mitophagy-dependent oxidative stress in human bronchial epithelial cells exposed to cigarette smoke extract (CSE). *J Food Biochem*. 2020;44:e13366.
41. Adenuga D, Yao H, March TH, Seagrave J, Rahman I. Histone deacetylase 2 is phosphorylated, ubiquitinated, and degraded by cigarette smoke. *Am J Respir Cell Mol Biol*. 2009;40:464–73.
42. Song H, Tao L, Chen C, Pan L, Hao J, Ni Y, et al. USP17-mediated deubiquitination and stabilization of HDAC2 in cigarette smoke extract-induced inflammation. *Int J Clin Exp Pathol*. 2015;8:10707–15.
43. Wu Z, Qiu M, Guo Y, Zhao J, Liu Z, Wang H, et al. OTU deubiquitinase 4 is silenced and radiosensitizes non-small cell lung cancer cells via inhibiting DNA repair. *Cancer Cell Int*. 2019;19:99.
44. Nakatsuka E, Sawada K, Nakamura K, Yoshimura A, Kinose Y, Kodama M, et al. Plasminogen activator inhibitor-1 is an independent prognostic factor of ovarian cancer and IMD-4482, a novel plasminogen activator inhibitor-1 inhibitor, inhibits ovarian cancer peritoneal dissemination. *Oncotarget*. 2017;8:89887–902.
45. Pavon MA, Arroyo-Solera I, Tellez-Gabriel M, Leon X, Viros D, Lopez M, et al. Enhanced cell migration and apoptosis resistance may underlie the association between high SERPINE1 expression and poor outcome in head and neck carcinoma patients. *Oncotarget*. 2015;6:29016–33.
46. Placencio VR, Ichimura A, Miyata T, DeClerck YA. Small Molecule Inhibitors of Plasminogen Activator Inhibitor-1 Elicit Anti-Tumorigenic and Anti-Angiogenic Activity. *PLoS One*. 2015;10:e0133786.
47. Chen Y, Yang C, Li Y, Chen L, Yang Y, Belguise K, et al. MiR145-5p inhibits proliferation of PMVECs via PAI-1 in experimental hepatopulmonary syndrome rat pulmonary microvascular hyperplasia. *Biol Open*. 2019;8:bio044800.
48. Wang X, Bustos MA, Zhang X, Ramos RI, Tan C, Iida Y, et al. Downregulation of the Ubiquitin-E3 Ligase RNF123 Promotes Upregulation of the NF- κ B1 Target SerpinE1 in Aggressive Glioblastoma Tumors. *Cancers (Basel)*. 2020;12:1081.
49. Boncela J, Przygodzka P, Papiewska-Pajak I, Wyroba E, Osinska M, Ciemniewski CS. Plasminogen activator inhibitor type 1 interacts with alpha3 subunit of proteasome and modulates its activity. *J Biol Chem*. 2011;286:6820–31.
50. Bhandary YP, Shetty SK, Marudamuthu AS, Midde KK, Ji HL, Shams H, et al. Plasminogen activator inhibitor-1 in cigarette smoke exposure and influenza A virus infection-induced lung injury. *PLoS One*. 2015;10:e0123187.
51. Zhang H, Liu B, Jiang S, Wu JF, Qi CH, Mohammadtursun N, et al. Baicalin ameliorates cigarette smoke-induced airway inflammation in rats by modulating HDAC2/NF- κ B/PAI-1 signalling. *Pulm Pharm Ther*. 2021;70:102061.
52. Tiwari N, Marudamuthu AS, Tsukasaki Y, Ikebe M, Fu J, Shetty S. p53- and PAI-1-mediated induction of C-X-C chemokines and CXCR2: importance in pulmonary inflammation due to cigarette smoke exposure. *Am J Physiol Lung Cell Mol Physiol*. 2016;310:L496–506.

ACKNOWLEDGEMENTS

The authors would like to thank all the participants involved in this study.

AUTHOR CONTRIBUTIONS

LJL and YC conceived and designed the research. LJL, TL, ZHZ, HRL, and XH performed experiments. LJL analyzed the data and drafted the manuscript. All authors reviewed and approved the final version of the manuscript.

FUNDING

This work was supported by the National Natural Science Foundation of China (No. 81873410 and 82070049), the Natural Science Foundation of Hunan Province (No.2022JJ30060), the Fundamental Research Funds for the Central Universities of Central South University (No. 2021zzts0369) and the Hunan Provincial Innovation Foundation for Postgraduate (CX20210371).

COMPETING INTERESTS

The authors declare no competing interests.

ADDITIONAL INFORMATION

Supplementary information The online version contains supplementary material available at <https://doi.org/10.1038/s41419-023-06131-1>.

Correspondence and requests for materials should be addressed to Yan Chen.

Reprints and permission information is available at <http://www.nature.com/reprints>

Publisher's note Springer Nature remains neutral with regard to jurisdictional claims in published maps and institutional affiliations.



Open Access This article is licensed under a Creative Commons Attribution 4.0 International License, which permits use, sharing, adaptation, distribution and reproduction in any medium or format, as long as you give appropriate credit to the original author(s) and the source, provide a link to the Creative Commons license, and indicate if changes were made. The images or other third party material in this article are included in the article's Creative Commons license, unless indicated otherwise in a credit line to the material. If material is not included in the article's Creative Commons license and your intended use is not permitted by statutory regulation or exceeds the permitted use, you will need to obtain permission directly from the copyright holder. To view a copy of this license, visit <http://creativecommons.org/licenses/by/4.0/>.

© The Author(s) 2023